Journal of Colloid and Interface Science 683 (2025) 1008–1018

Contents lists available at ScienceDirect

Journal of Colloid And Interface Science

journal homepage: www.elsevier.com/locate/jcis

Regular Article

Spontaneous formation of small and ultrasmall unilamellar vesicles in mixtures of drug surfactant and phospholipid: Effect of chemical structure of phospholipid tails on vesicle size

Vahid Forooqi Motlaq [a], Lars Gedda [b], Katarina Edwards [b], James Doutch [c], L. Magnus Bergström [a,*]

[a] Department of Medicinal Chemistry, Uppsala University, P.O. Box 547, 751 23, Uppsala, Sweden
[b] Department of Chemistry-Ångström, Uppsala University, P.O. Box 573, 751 23 Uppsala, Sweden
[c] ISIS Neutron and Muon Source, STFC, Rutherford Appleton Laboratory, Harwell Campus, Didcot, Oxon, UK

HIGHLIGHTS

- Vesicles can form spontaneously in the mixture of amphiphilic drugs and phospholipids.
- The effect of the tail chemical structure is more pronounced than the tail length.
- The different self-assembled aggregates can be rationalized by combining solution thermodynamics with bending elasticity theory.
- Ultra-small vesicles, smaller than 20 nm, were observed in the mixture of unsaturated phospholipids and amphiphilic drugs.

GRAPHICAL ABSTRACT

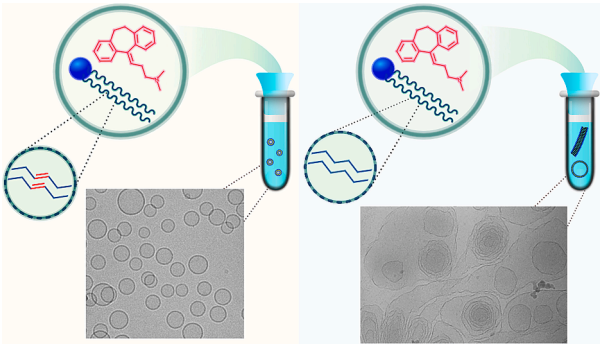

ARTICLE INFO

Keywords:
Vesicles
Micelles
Phospholipids
Drug surfactants
Small-angle scattering

ABSTRACT

We have investigated the effect of length and chemical structure of phospholipid tails on the spontaneous formation of unilamellar liposomal vesicles in binary solute mixtures of cationic drug surfactant and zwitterionic phosphatidylcholine phospholipids. Binary drug surfactant-phospholipid mixtures with four different phospholipids with identical headgroups (two saturated phospholipids 1,2-dimyristoyl-*sn-glycero*-3-phosphocholine (DMPC, 14:0) and 1,2-Dipalmitoyl-*sn-glycero*-3-phosphocholine (DPPC, 16:0), and two unsaturated lipids 1,2-dioleoyl-*sn-glycero*-3-phosphocholine (DOPC, 18:1) and 1,2-Dierucoyl-*sn-Glycero*-3-Phosphatidylcholine (DEPC, 22:1)) combined with two different tricyclic antidepressant drugs (amitriptyline hydrochloride (AMT) and doxepin hydrochloride (DXP)) have been investigated with small-angle neutron scattering (SANS) and cryo-transmission electron microscopy (cryo-TEM). We observe a conspicuous impact of phospholipid tail structure on both micelle-to-vesicle transition point and vesicle size. In particular, ultrasmall unilamellar vesicles, *i.e.* with a diameter less than 20 nm, were observed in several samples with the two unsaturated phospholipids DOPC and DEPC, but not in any samples with the saturated phospholipids DMPC and DPPC. The smallest vesicles observed in DOPC and DEPC mixtures were smaller than 18 nm in diameter. In contrast, the smallest vesicles observed in

* Corresponding author.
E-mail address: magnus.bergstrom@ilk.uu.se (L.M. Bergström).

https://doi.org/10.1016/j.jcis.2024.12.098
Received 24 July 2024; Received in revised form 7 November 2024; Accepted 15 December 2024
Available online 18 December 2024

DMPC mixtures were about 30 nm in diameter and always larger than 100 nm in DPPC mixtures. The ultrasmall vesicles showed exceptional colloidal stability. Moreover, bilayer vesicles predominated over micelles in a much wider range of concentrations for DOPC and DEPC mixtures as a result of having a smaller phospholipid mole fraction in the aggregates at the micelle-to-vesicle transition. Our results have been theoretically rationalized by combining solution thermodynamics with bending elasticity theory.

1. Introduction

Phospholipids usually form large multilamellar vesicles or other lamellar bilayer structures in aqueous solvents. Dispersions of small unilamellar vesicles, so-called liposomes, can be formed by sonication and extrusion of the phospholipid lamellar structures [1]. These liposome dispersions are not thermodynamically stable and degenerate as the size of the liposomes increases over time.

Alternatively, unilamellar vesicles may form spontaneously in certain surfactant-surfactant or surfactant-phospholipid mixtures [2–6]. Most notably in mixtures of two oppositely charged surfactants, and in the mixtures of bile salt and lecithin (technical mixture of phospholipids with identical phosphatidylcholine (PC) head group). In both cases, vesicles form spontaneously as mixed micellar solutions are diluted below a certain limit close to the critical micelle concentration (CMC) of the surfactant. The size of spontaneously formed unilamellar vesicles varies considerably from about 30 nm to more than 200 nm in diameter depending on the particular chemical system. In a few exceptional cases, vesicles even smaller than 20 nm in diameter have been observed [7].

We have recently discovered that unilamellar vesicles smaller than about 20 nm in diameter may form spontaneously when diluting solutions with mixed micelles formed by the cationic amphiphilic drug surfactant amitriptyline hydrochloride (AMT) and the zwitterionic phospholipid 1,2-dioleoyl-*sn-glycero*-3-phosphocholine (DOPC) in physiologic saline solution (PSS) at ambient temperature [8]. We observed a micellar region at concentrations well above the CMC of AMT. By simply diluting the samples below but close to the CMC of AMT, it was concluded that the driving force for structural transformations is a change in molecular composition in the aggregates caused by the presence of a significant amount of drug present as free monomers. Hence, we observed a region with mixed rodlike micelles that grow in size when diluting samples with molar ratios [AMT]/[DOPC] = 3 and 4 from [AMT] + [DOPC] = 40 to 20 mM. The micelles transform into small unilamellar vesicles upon further dilution below the CMC of AMT (=20 mM). Most interestingly, the vesicles were found to significantly decrease in size with decreasing concentration from about 60 nm in diameter at 20 mM to 15 nm at 5 mM. The solutions with vesicles smaller than 20 nm in diameter (ultrasmall vesicles) are stable as long we have observed them (several months) without any changes in vesicle size. This indicates that the systems are thermodynamically stable solutions, similar to micellar and microemulsion solutions, rather than kinetically stabilized dispersions.

In the present study, we follow up on our previous work to extend the investigation of the formation of small and ultrasmall unilamellar vesicles in drug surfactant-phospholipid mixtures. In particular, we investigate the impact of different phospholipid tail structure on the size and shape of aggregates formed by either of two cationic drug surfactants, amitriptyline hydrochloride (AMT) and doxepin hydrochloride (DXP), together with phospholipid. In our study, we have chosen four different phospholipids with a common phosphatidylcholine headgroup, two phospholipids with saturated tails (1,2-dimyristoyl-*sn-glycero*-3-phosphocholine (DMPC, 14:0) and 1,2-Dipalmitoyl-*sn-glycero*-3-phosphocholine (DPPC, 16:0)), and two phospholipids with unsaturated tails 1,2-dioleoyl-*sn-glycero*-3-phosphocholine (DOPC, 18:1) and 1,2-Dierucoyl-*sn-Glycero*-3-Phosphatidylcholine (DEPC, 22:1)).

1.1. Theory of spontaneous vesicle formation

The spontaneous formation of thermodynamically stable unilamellar vesicles can be rationalized by combining solution thermodynamics with bending elasticity theory [9]. The theory introduces three bending elasticity constants k_c (bending rigidity), H_0 (spontaneous curvature), and $\bar{k}_c$ (saddle-splay constant) that depends on the bending or curvature energy of the monolayer [10]. It follows that the vesicle size increases with increasing k_c, increasing $\bar{k}_c$ and decreasing k_cH_0 [9]. The dependence on spontaneous curvature can be rationalized as a result of the outer positively curved vesicle monolayer being more voluminous than, and dominating over, the negatively curved inner monolayer. The bending rigidity k_c is a measure of the ability of the surfactant monolayer to deviate from its spontaneous curvature. Hence, high values of k_c favors geometrically homogeneous aggregates, *i.e.* aggregates with small differences in local curvature. Since the difference in curvature between the outer and inner monolayers of a vesicle increases in magnitude with decreasing vesicle size, large k_c values favors large vesicles, and ultimately infinitely large planar bilayers, whereas the formation of small unilamellar vesicles is favored by small k_c values. Most interestingly, it has been demonstrated that k_c can be significantly reduced by mixing two surfactants, or a surfactant and a phospholipid [11–14], which is consistent with spontaneous vesicle formation only having been observed in surfactant-surfactant and surfactant-phospholipid mixtures. The saddle-splay constant has an impact on the equilibrium size of vesicles since it, similar to k_c, contributes with a size-independent term to k_{bi} and the vesicle bending energy. In accordance with Eq. (3), the vesicle size increases with increasing $\bar{k}_c$.

It has been shown that the mole fraction of phospholipid (x_{PL}) in mixed drug surfactant/phospholipid aggregates is generally different from the bulk solution (X_{PL}), especially at more dilute concentrations [15,16]. It is expected that the molar ratio of phospholipid inside the aggregates must be higher than in the overall solution ($x_{PL} > X_{PL}$). Upon dilution, particularly at concentrations below the CMC of the drug, an increasing amount of drug is leaving the aggregates to maintain free drug monomer concentration (and chemical potential) in solution. As a result, the deviation of x_{PL} from X_{PL} increases considerably in magnitude with decreasing amphiphile concentration below CMC of surfactant [8]. Moreover, we have previously shown that x_{PL} is more representative than X_{PL}, thus illuminating several properties of mixed micellar and vesicular systems [8,17]. Although, there is significant differences in CMC of the phospholipids used in the current study, the CMC for all phospholipids are several orders of magnitude smaller than CMC of the drug surfactants. Therefore, they virtually have no significant effect on x_{PL} in our calculations. More details about the calculations of the surfactant mole fraction in the aggregates are provided in the supplementary information section 6.

2. Materials and method

2.1. Materials

Amitriptyline hydrochloride (purity ≥ 98 %, abbreviated as AMT) and doxepin hydrochloride (purity ≥ 98 %, abbreviated as DXP) were purchased from Sigma-Aldrich, 1,2-dioleoyl-*sn-glycero*-3-phosphocholine (purity ≥ 98 %, 18:1, abbreviated as DOPC) and 1,2-Dierucoyl-*sn-Glycero*-3-Phosphatidylcholine (purity ≥ 98 %, 22:1, abbreviated as DEPC) were from Larodan AB, Sweden, and 1,2-dimyristoyl-*sn-glycero*-

3-phosphocholine (purity ≥ 98 %, 14:1, abbreviated as DMPC) and 1,2-Dipalmitoyl-*sn-glycero*-3-phosphocholine (purity ≥ 98 %, 16:1, abbreviated as DMPC) were from Lipoid AG, Steinhausen, Switzerland. All compounds were used as received without further purification. The chemical structures of these compounds are shown in Fig. 1.

Four different phospholipids and two amphiphilic drugs were combined in eight binary systems composed of one single phospholipid and one drug in physiological saline solution [NaCl] = 154 mM. The two components were simply swirled by magnet stirring overnight without using any external forces such as ultrasound, extrusion, etc. In the case of DMPC and DPPC samples, the overnight stirring was carried out at 37 °C. Deuterium oxide as a medium was used for both small-angle neutron scattering (SANS) and cryo-TEM measurements.

Each individual system was prepared in two dilution series with molar ratios of X_{PL} = [phospholipid]/([phospholipid] +[drug]) equal to 0.20 and 0.25. Dilution series were prepared from stock solutions with total concentration c_t = [phospholipid] + [drug] = 40 mM. The transparent stock solutions were further diluted to the corresponding total concentrations of the series ranging from 40 to 1 mM. All samples were prepared at least 72 h before and were left to equilibrate at 37°C for a minimum of 12 h prior to the measurements. For the sake of simplicity, we denote our samples throughout the text below using the following terminology [phospholipid-drug, molar ratio of phospholipid (X_{PL}), total concentration in mM (C_t)].

The gel-to-liquid crystalline phase transition temperature (T_g) for the unsaturated phospholipids DOPC and DEPC are −17 and 13 °C and for the saturated phospholipids DMPC and DPPC T_g equals 24 and 41°C, respectively. T_g of a drug-phospholipid mixture is lower than the phospholipid itself as a result of a phase transition point depression. For instance, the sample [DPPC-AMT, 0.25, 40] was observed to have a phase transition at about 29 °C. All the measurements in the current study were performed at 37 °C which is above T_g for all binary phospholipid-drug systems. Both amphiphilic drugs used, AMT and DXP, belong to the tricyclic anti-depressant drugs with a quite similar molecular structure. Both have surfactant properties and form micelles above their respective CMC [18]. Moreover, AMT and DXP have comparable CMCs, i.e. about 17 and 20 mM for AMT and DXP, respectively, in 154 mM NaCl.

2.2. Small angle neutron scattering (SANS)

Small angle neutron scattering (SANS) experiments were performed on the ZOOM instrument at ISIS neutron and muon spallation source at Rutherford Appleton Laboratory, Didcot, UK [19]. With the incident beam of 1.75–16.5 Å, and setting the sample to detector distance to 4 m, resulted in scattering vector moduli q ranging from 0.0042 to 0.84 $Å^{-1}$. The resolution in q ranges from 2.5 to 21 % from low to high q-values.

The Hellma quartz cells with a path length of 2 mm were used as sample containers. The measurements were performed at 37 °C and the samples were left to equilibrium for at least 12 h before the measurements. The background from the solvent, sample cell, and other sources was subtracted from the raw 2D images by conventional procedures [20]. Subsequently, the obtained images were reduced to 1D, normalized to the detector response, sample transmission, spectral, and wavelength distribution of the incident neutron beam using Mantid software [21]. After converting to absolute scale (in unit cm^{-1}), the SANS data were normalized by dividing with the solute concentration in [g cm^{-3}], giving normalized intensity in units [cm^2 g^{-1}]. Instrumental smearing corrections were found to have minimal effect on the fitting outcomes and were not explicitly considered in the fitting routine. Two

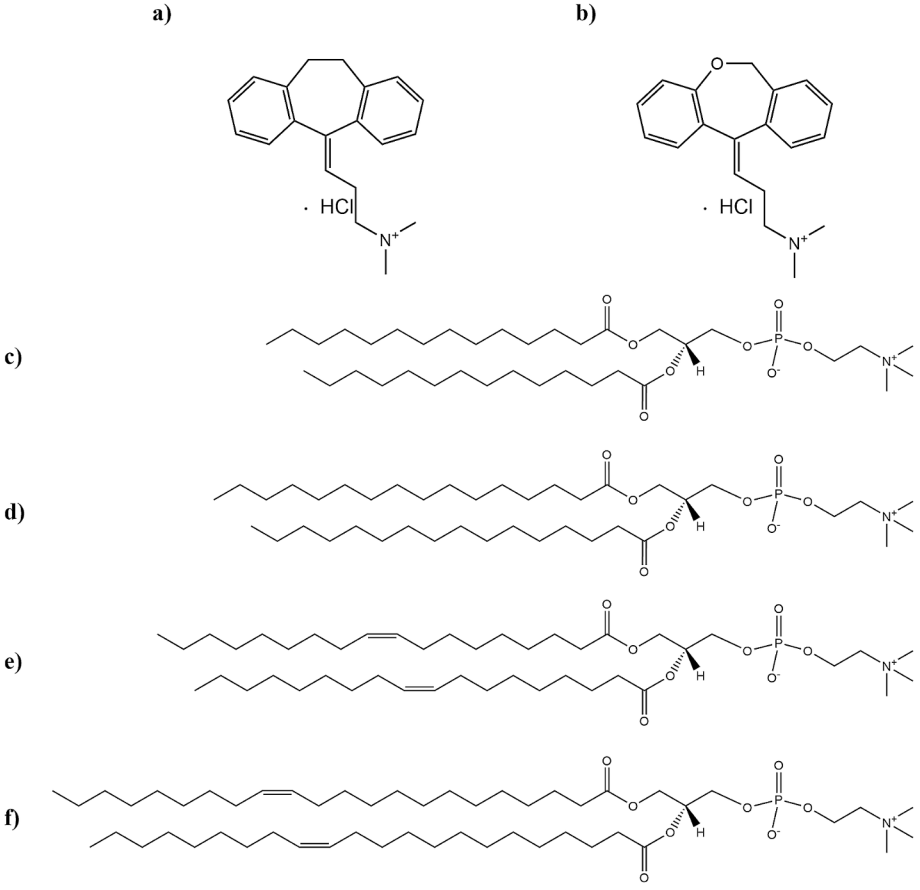

Fig. 1. Chemical structure of (a) amitriptyline (AMT), (b) doxepin (DXP), (c) 1,2-dimyristoyl-*sn-glycero*-3-phosphocholine (DMPC), (d) 1,2-Dipalmitoyl-*sn-glycero*-3-phosphocholine (DPPC), (e) 1,2-dioleoyl-*sn-glycero*-3-phosphocholine (DOPC), and (f) 1,2-Dierucoyl-*sn-Glycero*-3-Phosphatidylcholine (DEPC).

samples have not been measured due to the technical failure at the beamline [cf. Tables 1 and 2 below].

2.3. Cryogenic transmission electron microscopy (cryo-TEM)

Specimens for Cryogenic transmission electron microscopy (cryo-TEM) investigations were prepared at controlled temperature (37 °C) and humidity (>90 %) within a custom-built environmental chamber. A small drop (~1 μL) of the sample was deposited on a carbon-sputtered copper grid (300 mesh, Agar Scientific) covered with a perforated polymer film. Excess liquid was thereafter removed by blotting with a filter paper, leaving a thin film of the solution on the grid. The sample was then vitrified by plunging the grid into liquid ethane held at a temperature just above its freezing point, mounted in a sample holder, and transferred to the microscope. During the transfer and viewing processes, the sample was kept at a temperature below −160 °C and protected against atmospheric conditions. Analyses were performed with a Zeiss Libra 120 Transmission Electron Microscope (Carl Zeiss AG, Oberkochen, Germany) operating at 80 kV and in zero-loss bright-field mode. Digital images were recorded under low-dose conditions with a BioVision Pro-SM Slow Scan CCD camera (Proscan elektronische Systeme GmbH, Scheuring, Germany).

2.4. Data analysis of SANS data

An in-house least-squares fitting program developed by Pedersen et al. [22] was used to analyze the SANS data in a least-sqaure model fitting procedure. Different geometrical models were compared and the model that best described data for a particular sample was selected. Since all SANS measurements were carried out at relatively high electrolyte concentrations (154 mM NaCl), and relatively low aggregate concentration, the SANS data could be fitted with only a form factor without the need of implementing a structure factor into the models. Hence, it was not possible to obtain quantities such as the surface charge density and volume fraction of aggregates from a structure factor. The reduced chi-square was used as a measure of the quality of the fits and to distinguish between different models.

Our samples could be categorized into either of three main regions: 1) micelles formed at high total amphiphile concentration, 2) coexistence of micelles with vesicles/disks formed at intermediate concentrations, and 3) vesicles/disks formed in the most dilute solutions. Data for samples with the smallest micelles were best fitted with a model for monodisperse triaxial ellipsoidal micelles. Data for samples with larger micelles were best fitted with a model for elongated rigid rodlike micelles with an elliptical cross-section that are considerably polydisperse with respect to length. When stiff rodlike micelles grow longer they eventually become more flexible and the quality of the model fits could be significantly improved using a form factor for flexible wormlike micelles in our data analysis. In some of our samples, the micelles were too large for their contour length to be determined from our SANS data, and only the cross-section parameter is reported.

For samples just below the micelle-to-bilayer transition point, different aggregate types (micelles, vesicles, disks) may coexist together (see below for further discussion). These samples were fitted with a model with form factors for rodlike micelles, vesicles, and disks, and no core–shell structures were implemented in the model. The micelle-bilayer coexistence model was only used if no reasonable quality of the fit was obtained assuming only vesicles and disks in the sample. Micelles and bilayer aggregates were seen to coexist in five of our samples.

Upon dilution the systems pass the point of micelle to bilayer transition and eventually no micellar aggregates exist in the samples. For these dilute samples in the bilayer region, the SANS data were best fitted with a model for polydisperse vesicles or a model for coexisting polydisperse vesicles and monodisperse open bilayer disks. The quality of the model fits were slightly improved by means of taking into account the core–shell nature of the bilayers. In samples containing bilayer vesicles, the presence of disks were only taken into account in so far the quality of the model fit as measured with chi-squared was significantly improved. In some of our samples, the bilayer aggregates are too large for their size to be determined from our SANS data and it is no longer possible to distinguish between disks and vesicles. Hence, for these samples only the bilayer cross-section structure and dimensions could be determined.

The general approach during the model fitting analysis was to keep

Table 1
Summary of the models used in the Small-Angle Neutron Scattering (SANS) data analysis for the binary mixture of amitriptyline with different phospholipids sorted gradationally for the calculated composition of phospholipid fraction inside the aggregates (x_{PL}). First column shows the composition (mole fraction of phospholipid) in bulk solution (X_{PL}) and total concentration (C_t).

$X_{PL} - C_t$/mM	x_{PL}	DMPC	DPPC	DOPC	DEPC
0.20-40	0.29	Tri-axial micelle	Tri-axial micelle	Rodlike micelle	Rodlike micelle
0.20-30	0.33	Rodlike micelle	Tri-axial micelle	Rodlike micelle	Rodlike micelle
0.25-40	0.35	Rodlike micelle	Rodlike micelle	Rodlike micelle	Vesicles + Disks + Rodlike micelles
0.25-30	0.39	Rodlike micelle	Rodlike micelle	Vesicles + Disks + Rodlike micelles	Vesicles + Disks + Rodlike micelles
0.20-20	0.42	Rodlike micelle	Rodlike micelle	Vesicles + Disks + Rodlike micelles	Vesicles + Disks
0.25-20	0.47	Rodlike micelle	Wormlike micelle	Vesicles + Disks	Vesicles + Disks
0.20-10	0.62	Vesicles + Disks	Bilayers	Vesicles + Disks	Vesicles
0.25-10	0.65	Bilayers	Bilayers	Vesicles + Disks	Vesicles
0.20-5	0.79	Vesicles	Bilayers	Not measured	Vesicles
0.25-5	0.81	Vesicles	Bilayers	Vesicles + Disks	Vesicles + Disks
0.20-1	0.95	Vesicles + Disks	Bilayers	Bilayers	Vesicles + Disks
0.25-1	0.96	Vesicles + Disks	Bilayers	Bilayers	Vesicles + Disks

Table 2
Summary of the models used in the Small-Angle Neutron Scattering (SANS) data analysis for the binary mixture of doxepin with different phospholipids sorted gradationally for the calculated composition of phospholipid fraction inside the aggregates (x_{PL}). First column shows the composition (mole fraction of phospholipid) in bulk solution () and total concentration (C_t).

$X_{PL} - C_t(mM)$	x_{PL}	DMPC	DPPC	DOPC	DEPC
0.20-40	0.31	Rodlike micelle	Rodlike micelle	Vesicles + Disks + Rodlike micelles	Vesicles + Disks
0.20-30	0.35	Wormlike micelles	Wormlike micelles	Vesicles + Disks	Vesicles + Disks
0.25-40	0.37	Rodlike micelle	Wormlike micelles	Vesicles + Disks	Vesicles + Disks
0.25-30	0.41	Not measured	Vesicles + Disks	Vesicles + Disks	Vesicles + Disks
0.20-20	0.45	Bilayers	Bilayers	Vesicles + Disks	Vesicles + Disks
0.25-20	0.50	Bilayers	Bilayers	Vesicles + Disks	Vesicles + Disks
0.20-10	0.65	Vesicles + disks	Bilayers	Vesicles + Disks	Vesicles
0.25-10	0.68	Vesicles + Disks	Bilayers	Vesicles + Disks	Vesicles
0.20-05	0.81	Vesicles	Bilayers	Vesicles + Disks	Vesicles + Disks
0.25-05	0.83	Vesicles	Bilayers	Vesicles + Disks	Vesicles + Disks
0.20-01	0.96	Bilayer	Bilayers	Bilayers	Vesicles + Disks
0.25-01	0.96	Bilayer	Bilayers	Bilayers	Vesicles + Disks

the model as simple as possible and additional fitting parameters were only introduced if the quality of the fits could be significantly improved. More details of the employed models and fitting results from our data analysis are provided in the Supplementary information.

3. Results and discussion

3.1. Small-angle neutron scattering

The models generating best agreement with SANS data for the different samples are summarized in Tables 1 and 2. The results are sorted against the mole fraction of phospholipid in the aggregates (x_{PL}). x_{PL} was calculated from a model based on solution thermodynamics as described above and shown in Table S6 in Supplementary information. Detailed results from the SANS data analysis are summarized in Tables S1–S4 in the Supplementary information.

Aggregate type denoted "vesicles" or "vesicles + disks" means that the vesicles and disks are sufficiently small for their size to be determined from the SANS measurements. Samples denoted "bilayers" mean that the bilayer aggregates are too large for their size to be determined with SANS. In these samples, the typical oscillation in the scattering curves, indicating the presence of vesicles in a sample, is located below the lower limit of accessible q and, hence, could not be observed in our data. This means that it is not possible to distinguish between vesicles and disks. Only parameters related to bilayer thickness were reported in Tables S1–S4 for these samples.

There is an obvious correlation between x_{PL} and aggregate type. Micelles are formed at smaller values of x_{PL}, that is at higher fractions of drug surfactant in the aggregates, whereas various bilayer aggregates are the predominant aggregate type at higher values of x_{PL}. In between, there is a rather narrow regime of x_{PL} where micelles coexist with vesicles and disks.

3.1.1. Micellar region

The smallest micelles observed were less than 10 nm in length direction and found at high concentrations in the samples [DMPC-AMT, 0.20, 40] and [DPPC-AMT, 0.20, 40]. The corresponding SANS data were fitted with a model for monodisperse general ellipsoids with half-axes a, b, and c (indicating the presence of micelles with distinctive length > width > thickness). Cryo-TEM images for the sample [DPPC-AMT, 0.25, 40] are shown in Fig. S13 in the Supplementary information. The formation of the triaxial micelles has previously been rationalized by the general micelle theory [23,24]. The length of the micelles is seen to grow with increasing x_{PL} and, eventually, a model for polydisperse elongated rodlike micelles with an elliptical cross-section could generate better quality of the model fits. According to the general micelle model, the size and geometry of micelles depend on bending elasticity properties, as well as on total surfactant/phospholipid concentration [24,25]. Rather small compact micelles may grow (in length dimension) into long rodlike or wormlike micelles above the second critical micelle concentration (2nd CMC). Since the 2nd CMC decreases significantly with increasing x_{PL}, larger micelles tend to form close to the micelle-to-bilayer transition. As rodlike micelles grow longer than about the persistence length, they transform into more flexible wormlike micelles [24]. In each individual binary mixture of drug and phospholipid, we observed an associated growth in the size of the micelles as x_{PL} increases. Fig. 2 shows SANS data with model fits, for a sequence of samples where micelles grow from small monodisperse triaxial micelles, via polydisperse rigid rodlike micelles, to flexible wormlike micelles in various mixtures of DPPC and AMT. Wormlike micelles were observed in the sample [DPPC-AMT, 0.25, 20] with an aggregate compositionx_{PL} = 0.47. This was the sample with highest x_{PL} that contains micelles without any bilayer aggregates, occurring just before the point of micelle-to-bilayer transition. The presence of flexible wormlike micelles is characterized by a point of inflection in the scattering data, and the SANS data were fitted with a model of self-avoiding Kratky-Porod wormlike chains with an average contour length $\langle L \rangle$ and persistence length l_p [26]. While the micelles grow in length upon dilution, the cross-section dimensions remained virtually the same throughout the series and are consistent with previous reports [27,28]. The largest micelles observed are too large for their length and polydispersity to be determined from our SANS data, and only parameters related to cross-section dimensions are reported for these samples in Tables S1–S4.

The chemical structures of AMT and DXP only differ in that a cyclic methylene group in AMT is exchanged for an oxygen in DXP. For this reason, the more hydrophilic DXP has a slightly higher CMC than AMT.

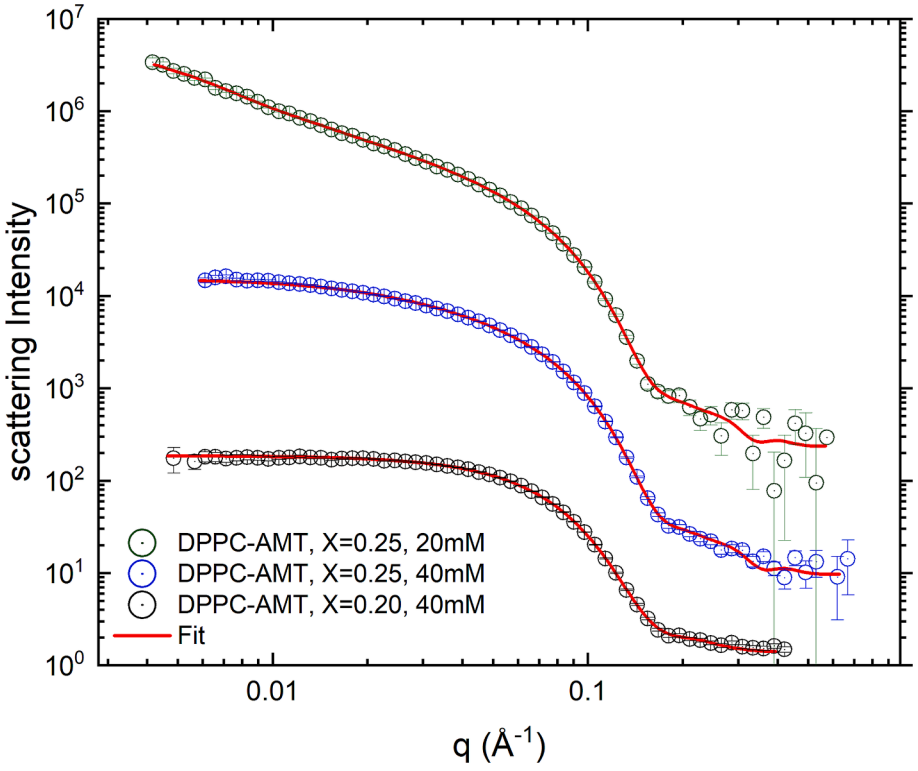

Fig. 2. SANS curves and their corresponding fits for three samples from DPPC-AMT binary system in the micellar region. [DPPC-AMT, 0.20, 40] sample (x_{PL} = 0.29) fitted with triaxial ellipsoid model, [DPPC-AMT, 0.25, 40] sample (x_{PL} = 0.35) fitted with rodlike model, and [DPPC-AMT, 0.25, 20] sample (x_{PL} = 0.47) fitted with wormlike model, demonstrated in top, middle, and bottom panels, respectively. This is an example of transformation from triaxial to rodlike and eventually to wormlike micelle upon lowering the total concentration. Plots are scaled in arbitrary units for the purpose of visualization.

Consequently, among samples with identical total concentration and composition, there are fewer samples found in the micellar region for systems with DXP. Comparing samples with different drug, but identical phospholipid mole fraction in the aggregates (x_{PL}), we find that mixed DXP-phospholipid micelles are somewhat larger than the corresponding AMT mixed micelles. Likewise, wormlike micelles that are too large for their size to be determined from our SANS data are more frequently observed in the DXP-systems as compared with AMT. Moreover, at a specific aggregate composition, micelles formed in mixtures with an unsaturated phospholipid (DOPC or DEPC) are considerably larger as compared to those formed in mixtures with a saturated phospholipid (DMPC and DPPC). This might be rationalized as a consequence of the former phospholipids having longer tails, lower hydrophilic-lipophilic balance and lower spontaneous curvature.

3.2. *The transition from micelles to bilayer structures*

All binary mixtures of both drugs at a sufficiently low total concentration (C_t) reach a point where the scattering data is no longer consistent with the presence of only micelles. Below this point, the SANS data were best fitted with some kind of bilayer model. In a few intermediate samples in both DXP and AMT systems, the quality of the fits could be significantly improved by using a model for coexisting micelles, vesicles, and disks.

For each binary drug-phospholipid system, we can estimate a range of phospholipid mole fractions ranging from the highest x_{PL} where only micelles are observed to the lowest x_{PL} where only bilayer aggregates are observed, indicating the point of transition from micelles to bilayers. Our results are summarized in Table 3. In the AMT series, the transition region is about the same for both saturated phospholipids (DMPC and DPPC), while the point of transition for unsaturated phospholipids (DOPC and DEPC) is located at considerably lower values. Moreover, the transition for the DEPC systems occurs at lower x_{PL} compared with DOPC systems. For the systems with DXP mixed with either DOPC or DEPC, this point of transition was located beyond the highest measured concentration and bilayers were observed in all samples up to C_t = 40 mM. For the two saturated phospholipids mixed with AMT and DXP, we never observed micelles and bilayers coexisting in any of our samples indicating a more abrupt transition from micelles to bilayers in binary mixtures with DMPC and DPPC.

Table 3
The range that micelle-to-bilayer transition happens for each individual binary system. For the doxepin-DOPC/DEPC mixtures, the point of transition were beyond the range of our experiments.

AMT		DXP	
Lipid	x_{PL}	*Lipid*	x_{PL}
DMPC (14:0)	0.47–0.62	DMPC	0.37–0.45
DPPC (16:0)	0.47–0.62	DPPC	0.37–0.41
DOPC (18:1)	0.35–0.39	DOPC	~0.3
DEPC (22:1)	0.33–0.35	DEPC	<0.3

We have previously shown that the point of micelle-to-bilayer transition depends on the spontaneous curvature (H_0) of the amphiphilic components. More specifically, micelles predominate as $H_0 > 1/4\xi$ and bilayer aggregates as $H_0 < 1/4\xi$, where ξ is the monolayer thickness [29]. Thus, the presence of micelles is favored by high values of k_cH_0 (effective spontaneous curvature) and low values of k_c (bending rigidity), whereas bilayer aggregates are favored by low values of k_cH_0 and high values of k_c [17]. Comparing the point of transition from micelles to bilayers in terms of x_{PL} in Table 3, we may qualitatively rank H_0 for the different phospholipids in our study in the following sequence [DPPC and DMPC] > DOPC > DEPC. This sequence is consistent with H_0 increasing with increasing hydrophilic-lipophilic balance (HLB) of the phospholipid. However, the situation might be more complicated and it

has been estimated that the spontaneous curvature of DPPC (16:0) is lower than for both DMPC (14:0) and DSPC (18:0) [30]. Notably, the point of transition for all phospholipids mixed with DXP occurs at lower values of x_{PL} compared with the corresponding AMT mixtures. This suggests that the spontaneous curvature of DXP is lower than for AMT.

3.3. The bilayer region

At concentrations below the micelle-to-bilayer transition, vesicles and disks usually coexist in all binary mixtures. The size of the bilayer aggregates is comparatively large in the coexistence region but decreases significantly upon dilution. Most interestingly, there are notable differences between the different phospholipids. As mentioned above, bilayer aggregates predominate in a wider range of concentrations for the two unsaturated phospholipids (DOPC and DEPC) as compared to the saturated phospholipids (DMPC and DPPC). Moreover, unilamellar vesicles appear to be considerably smaller in mixtures with unsaturated phospholipids than in mixtures with saturated phospholipids.

3.3.1. Binary mixtures with DOPC and DEPC

Fig. 3a shows the SANS curves for the [DEPC-DXP, 0.25] series. In this series, SANS data for all samples could be fitted with a model for coexisting vesicles and disks or a model for only vesicles. The presence of vesicles, with a bilayer shell structure, in a sample gives rise to a typical oscillation in the scattering data. The average size of the vesicles can be determined from the location in q of this oscillation. In Fig. 3a, vertical arrows indicate the start of the oscillation for each sample. It is evident that with a decrease in C_t, from 40 to 5 mM, the oscillation systematically shifts toward higher q values, indicating a reduction in the radius of the vesicles with decreasing concentration. The vesicles appear to assume a minimum size at 5 mM, where they start to grow in size upon further dilution to 1 mM. Fig. 3b shows the vesicle radius plotted against the total concentration for four binary mixtures with DEPC. All series show a minimum vesicle size at the very same total concentration equal to 5 mM. Similar behaviors can also be observed in the four DOPC-DXP dilution series (cf. Table S5 and Fig. S10).

Ultrasmall vesicles, i.e. vesicles with radius less than 10 nm could be observed in all four binary systems with unsaturated phospholipid (DOPC-AMT, DOPC-DXP, DEPC-AMT, and DOPC-DXP). The smallest vesicles were observed in the samples [DOPC-DXP, 0.25, 5] and [DOPC-DXP, 0.20, 5] with a vesicle (bilayer midplane) radius equal to about 6.5 nm at 37 °C [cf. Fig. 4]. This is somewhat smaller than the previously reported value, equal to 6.8 nm, for the sample [DOPC-AMT, 0.25, 5] at 22 °C. Cryo-TEM images of ultrasmall vesicles are shown in Fig. 5 for the samples [DEPC-AMT, 0.25, 10] and [DEPC-AMT, 0.25, 5]. Nearly spherical vesicles are observed at 10 mM, whereas even smaller, and obviously non-spherical, vesicles are shown at 5 mM.

We may also note that the vesicle size in the micelle-vesicle/disk coexistence region at 30 and 40 mM for the dilution series [DEPC-AMT, 0.25] is virtually identical as compared to the size at 20 mM in the same series, in which no micelles and only vesicles/disks are present (cf. Fig. 3b]. This is evident from our SANS data where the oscillation is located at virtually the same q-value for these three samples (cf. Fig. S2).

3.3.2. Binary mixtures with DMPC and DPPC

Compared with DOPC and DEPC, there are fewer samples in the DMPC binary mixtures that contain vesicles small enough for their size to be determined with SANS, *i.e.* smaller than about 50 nm in radius. A similar trend as observed for the DOPC and DEPC systems, *i.e.*, decreasing vesicle size upon dilution and a minimum size at a total concentration of 5 mM, could also be seen in the DMPC-drug systems. Notably, the formation of ultrasmall vesicles (radius smaller than 10

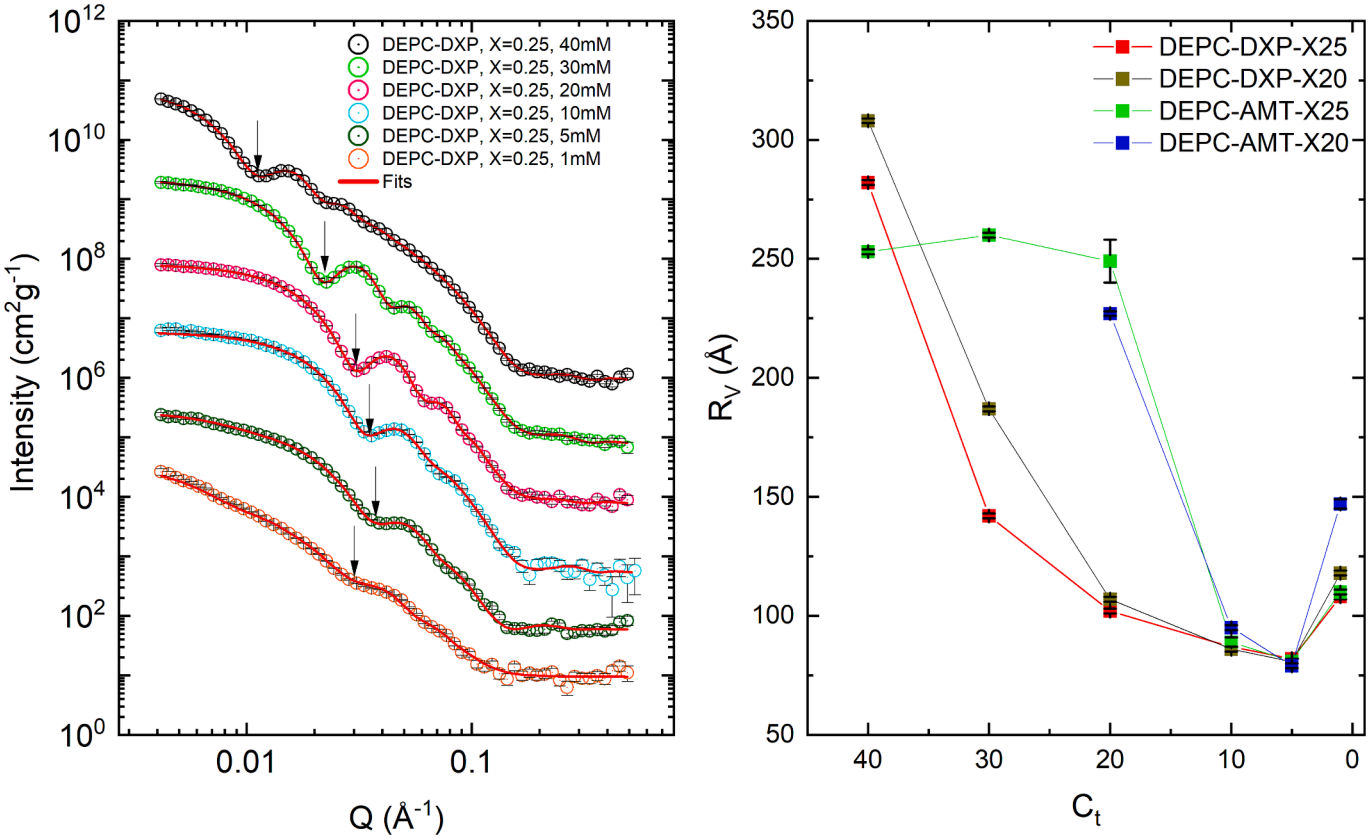

Fig. 3. Illustration of fitted SANS curves for the [DEPC-DXP, 0.25] series (left). The arrows show the place of minima for first oscillation. Plots are scaled for purpose of visualization. The right panel shows the plot of vesicle sizes (for the samples that contained vesicle) vs total concentration, for DEPC series with both amitriptyline and doxepin, at both compositions of X_{PL} = 0.20 and 0.25 for each drug.

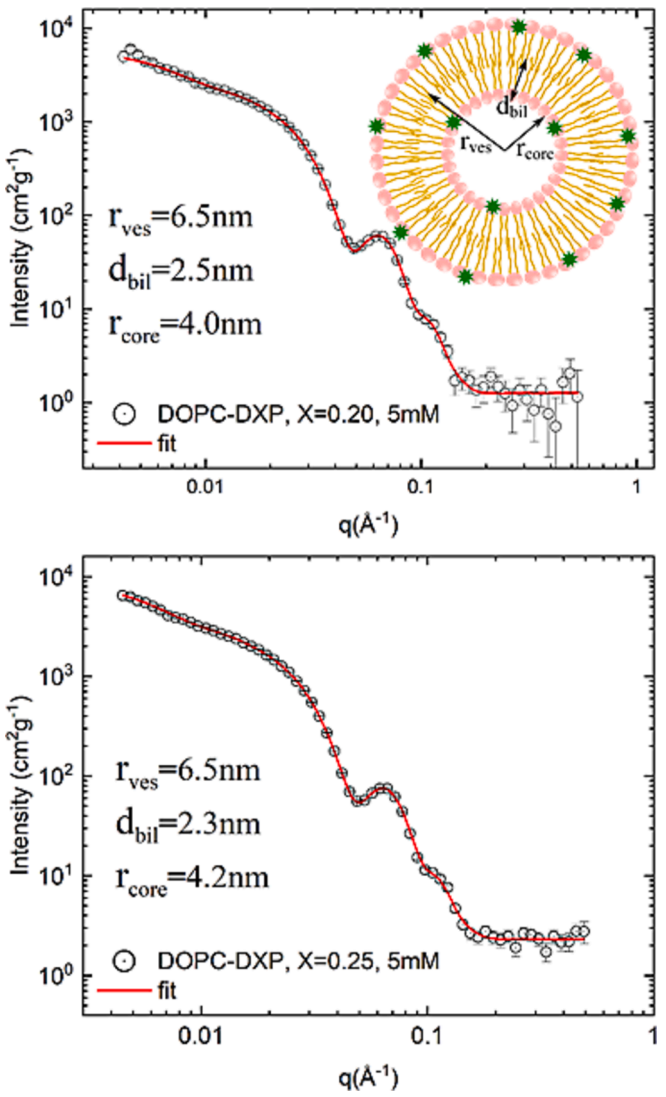

Fig. 4. Illustration of fitted SANS curves for the samples [DOPC-DXP, 0.20, 5] (top), and [DOPC-DXP, 0.25, 5] (bottom). Both samples contain ultrasmall vesicles with radii of 6.5 nm and core radii around 4 nm coexisting with a certain amount of larger disks. The contribution from the disks is mainly observed in the lowest q regime below about 0.01 $Å^{-1}$. The complete results from the model fitting analysis is shown in Table S3. A schematic representation of an ultrasmall vesicle is shown on top.

nm) was never observed in any mixtures with DMPC. Bilayer aggregates formed in DPPC-drug mixtures is found to be even larger than in the DMPC-drug mixtures. As a matter of fact, the bilayer aggregates were always seen to be too large for their size to be determined with SANS (R_v > 50 nm). Hence, we may conclude that the chemical structure of phospholipid has a very large impact on the size of spontaneously formed vesicles. Ultrasmall vesicles with a radius below 10 nm are only observed to form with the two unsaturated phospholipids DOPC and DEPC. The size of unilamellar vesicles formed by saturated phospholipids depends strongly on the length of the phospholipid tails and increases in size with increasing tail length.

3.4. Rationalizing the size of spontaneously formed vesicles with bending elasticity theory

In accordance with Eqs. (S25) and (S26), the size of spontaneously formed vesicles is expected to increase with decreasing effective spontaneous curvature (k_cH_0), increasing bending rigidity k_c and increasing saddle-splay constant $\bar{k}_c$. The effective spontaneous curvature favors smaller vesicles mainly because the positively curved outer layer is more voluminous, with a larger number of molecules, dominating over the less voluminous and negatively curved inner layer. Large values of the bending rigidity favor smaller deviations in curvature between different geometrical parts of an aggregate. Hence, small vesicles, with a larger difference in curvature between the positively curved outer layer and the negatively curved inner layer, are favored by small k_c values. In addition, the bending rigidity is expected to influence the shape of vesicles in so far small k_c values favor deviations from a spherical shape. The saddle-splay constant has an impact on the number of aggregates formed. Low values of $\bar{k}_c$ favors a large number of smaller vesicles whereas high $\bar{k}_c$ favors few larger bilayer aggregates. In addition to the three bending elasticity constants, the vesicle size is determined by the concentration of amphiphilic components in terms of volume fraction of bilayer aggregates. The aggregation number is proportional to ϕ_{ves} and $R_v \propto \phi_{ves}^{1/2}$.

As mentioned above, the transition from micelles to bilayer aggregates is mainly determined by the spontaneous curvature in so far that micelles predominates as $H_0 > 1/4\xi$ and bilayers as $H_0 < 1/4\xi$, where ξ is the thickness of the surfactant monolayer. According to the results in Table 3, we may thus conclude that the spontaneous curvature is larger for the two saturated phospholipids, DMPC and DPPC, than for the unsaturated phospholipids, DOPC and DEPC, with bigger tails. Since $H_0 = k_cH_0/k_c$, a large H_0 may either be due to large effective spontaneous curvature k_cH_0 or small k_c, or possibly both. Hence, we may conclude that the smaller vesicles found in mixtures of DOPC and DEPC cannot be rationalized by differences in spontaneous curvature, but rather by smaller values of the bending rigidity or, possibly, saddle-splay constant.

It has been demonstrated that the three bensing elasticity constants k_cH_0, k_c and$\bar{k}_c$ can be written as a sum of two contributions [31]. One contribution takes into account curvature properties of an infinitelty thin monolayer and the other contribution comprises effects due to the monolayer having a finite thickness largely determined by chain conformational entropy effects of flexible surfactant/lipid tails. The finite thickness effects contributes with a negative term to k_cH_0 and a postitive term to k_c. Most interestingly, for surfactants and amphiphilic lipids with completely rigid tails, the finite thickness terms are missing giving higher effective spontaneous curvature and lower bending rigidities compared with flexible tails at identical monolayer thickness.

Since the double bond of the two unsaturated phospholipids significantly reduces the flexibility of the tail part of DOPC and DEPC, the bending rigidity is expected to be lower for the systems with unsaturated phospholipids. This could explain the conspicuously smaller vesicles formed in the DOPC and DEPC systems. Low k_c values is also expected to favor a non-spherical shape of the vesicles. The observation in cryo-TEM that ultra-small vesicles at low concentrations frequently deviate from spherical shape also indicates that the bending rigidity is particularly low in mixtures with unsaturated phospholipid. By comparing the minimum size of vesicles for each phospholipid, it is indicated that the bending rigidity of the investigated phospholipids may be ranked according to the following trend: DOPC ≤ DEPC < DMPC < DPPC.

Furthermore, in the case of mixing two amphiphilic components a third term appears in the expression for k_c, which is absent in the corresponding expressions for k_cH_0 and$\bar{k}_c$ [14]. This contribution is found to be always negative. As a result, the bending rigidity becomes reduced by mixing two components with different preferences in curvature so that one of the components (surfactant) prefers to be located in the outer vesicle monolayer whereas the other (phospholipid) prefers the inner layer. The larger asymmetry between drug surfactant and phospholipid with bigger tail (DOPC and DEPC) may have enhanced the reduction of k_c. The minimum size of the unilamellar vesicles at a certain concentration (corresponding to a certain composition in the vesicles), as observed in Fig. 3, may be the result of an optimal drug-phospholipid composition where the bending rigidity reaches a minimum. In all

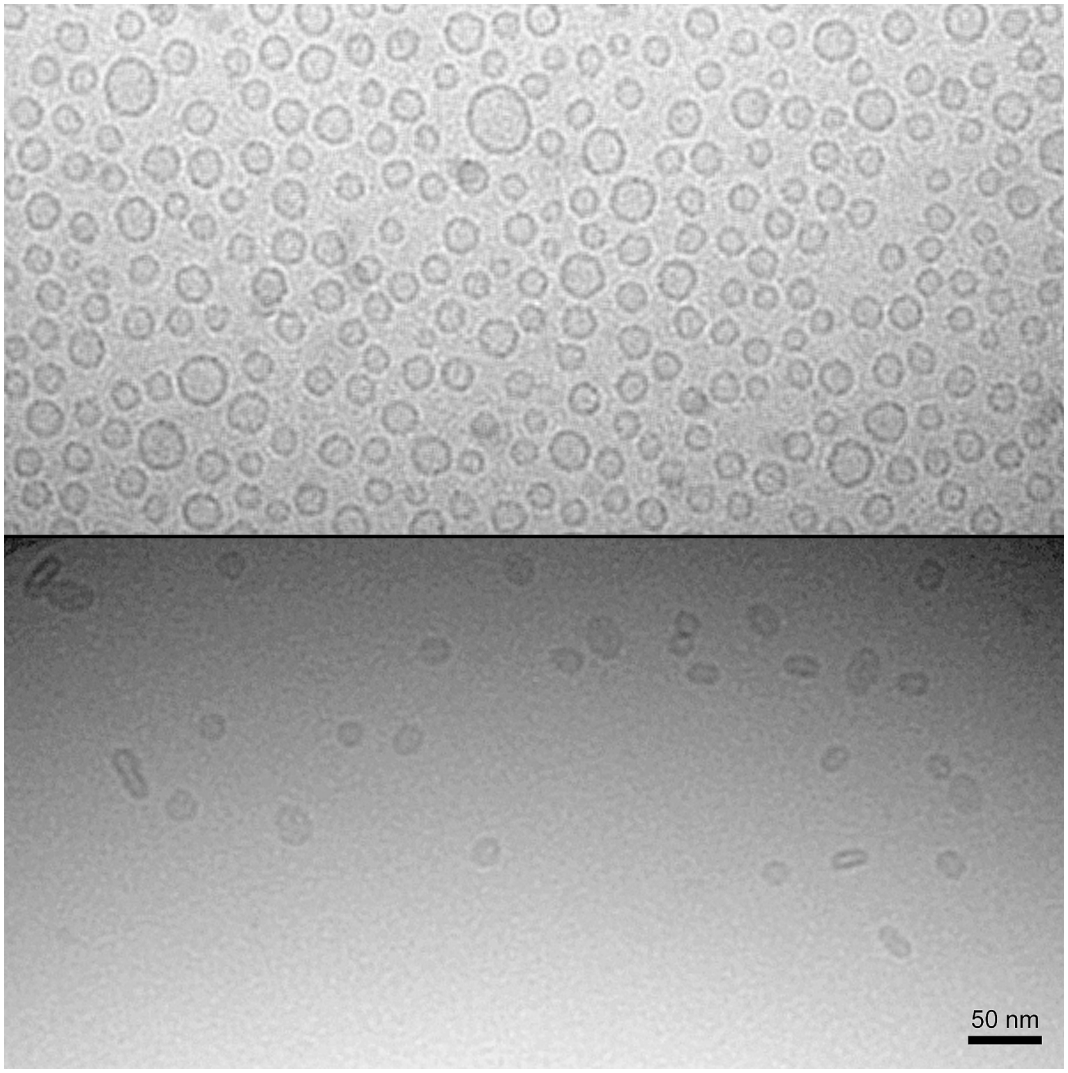

Fig. 5. Cryo-TEM image of the [DEPC-AMT, 0.25, 10] sample (top panel), and cryo-TEM images for [DEPC-AMT, 0.25, 5] sample (middle and bottom panels). The scale bar is 50 nm and constant for all pictures. The arrows v and d show a vesicle and a disk, respectively.

binary drug-phospholipid mixtures, a minimum vesicle size is reached at 5 mM total amphiphile concentration. This concentration corresponds to a rather high mole fraction of phospholipid in the vesicles, *i.e.* x_{PL} equal about 0.8 according to our model calculations [cf. Tables 1 and 2]. As a matter of fact, according to previous model calculations the reduction of k_c is enhanced when mixing a single-tail ionic surfactant with a double-tail nonionic surfactant (resembling our currently studied systems) as compared with a single-tail ionic and a single-tail nonionic surfactant [14]. Moreover, the minimum in mixing contribution to k_c was shifted to higher fractions of nonionic surfactant in the former case. In addition to bending elasticity effects, the decreasing vesicle size upon dilution may have been enhanced by the concentration dependence of the vesicle size.

3.5. Effect of temperature on bending elasticity constants

Recently, we investigated the DOPC-AMT system at room temperature [8] and it is interesting to compare the results with the present study carried out at 37 °C. It appears that the amount of open disks coexisting with unilamellar vesicles is higher at higher temperatures. For instance, only vesicles were observed in the sample [DOPC-AMT, 0.25, 5] at room temperature, whereas a substantial amount of disks (about 72 %) were present at 37 °C (*cf.* Tables S1 and S2). Moreover, the point of transition from micelles to bilayers has shifted to lower phospholipid content with increasing temperature, *i.e.* from x_{PL} = 0.42–0.47 at 22℃ [8] to x_{PL} = 0.35–0.39 at 37 °C.

This could be explained by the fact that the spontaneous curvature H_0 (k_cH_0/k_c) of the system, is reduced as the temperature increases. The findings are consistent with previous reports demonstrating that H_0 for DOPC decreases with increasing temperature, and $\frac{dH_0}{dT}$ has a negative slope at the temperature range of our experiments [32,33]. In addition, our previous results showed that the spontaneous curvature for bile salts decreases with an increase in temperature [17]. The amphiphilic drugs have a structure similar to that of bile salts, consisting of a rigid tail and a small ionic headgroup, suggesting the spontaneous curvature of AMT and DXP may drop with an increase in temperature.

Moreover, in the previous study at ambient temperature, the smallest vesicles (radius 8.1 nm) were found for the sample [DOPC-AMT, 0.25, 5]. At 37 °C, the smallest vesicles (radius 6.8 nm) were observed in the very same sample [cf. Tables S1 and S2 in Supplementary information]. The decrease in size at elevated temperatures indicates that the bending rigidity of the system is influenced by temperature, shifting towards lower values with an increase in temperature. This is in agreement with previous reports for DOPC [34]. These observations highlight a substantial temperature dependence of the various bending elasticity parameters for this kind of lipid systems.

4. Conclusions

It is well-known since decades that phospholipids may be dissolved by conventional detergents or bile-salt surfactants into mixed micelles beyond a certain threshold of surfactant concentration [4,6]. Bile salts have been observed to be particularly efficient in forming mixed micelles with a high phospholipid content [5,6]. Moreover, diluting bile salt-phospholipid mixed micelle solutions frequently generate a transition from micelles to small unilamellar vesicles [3]. More recently, it was demonstrated that a phospholipid could be dissolved by the drug surfactant AMT into mixed micelles and that small unilamellar vesicles formed spontaneously upon the dilution of the samples [8]. It was also discovered that the vesicles formed in the AMT-DOPC system were much smaller than previously reported for any surfactant-phospholipid system. The liposomal vesicles could have a diameter as small as less than 20 nm and we have denoted them ultrasmall vesicles.

Although surfactant-phospholipid mixtures have been studied for decades, the impact of phospholipid chemical structure on the properties of micelles and vesicles is less known. No systematic studies of the impact of choice of phospholipid on, for instance, the size of spontaneously formed vesicles, have previously been carried out. In the present article, we have followed up on our recent discovery and investigated the impact of phospholipid tail length and chemical structure on the structural behavior in various binary mixtures of drug surfactant (AMT or DXP) and phospholipid (DMPC, DPPC, DOPC, or DEPC) in physiological saline solution at human body temperature. In all binary solute mixtures, mixed micelles form at sufficiently high total concentrations that transform abruptly upon dilution to bilayer vesicles and disks below a critical concentration limit. The point of transition in terms of the mole fraction of phospholipid in the aggregates (x_{PL}) decreases with increasing size of the phospholipid hydrophobic tails. Above the critical concentration limit, rather small ellipsoidal or rodlike micelles grow in size upon dilution to large rigid rodlike or flexible wormlike micelles.

Most interestingly, there is a conspicuous difference in structural behavior in the bilayer region between the two unsaturated phospholipids (DOPC and DEPC), on the one hand, and the two saturated phospholipids (DMPC and DPPC), on the other hand. First, the region of concentrations where bilayer aggregates predominate over micelles is considerably wider for the unsaturated lipids. This reflects a difference in the point of the micelle-to-bilayer transition. Thus, the transition occurs at an aggregate mole fraction $x_{PL} = 0.5$–0.6 in the case of saturated lipids, while it is shifted to 0.35–0.4 in the case of unsaturated lipids. Second, the spontaneously formed unilamellar vesicles are significantly smaller in mixtures with unsaturated phospholipids. Ultrasmall vesicles are formed by both drug surfactants in binary mixtures together with DOPC and DEPC at total concentrations of 5 and 10 mM. A minimum radius of the ultrasmall vesicles in the range of 6.5–8 nm is obtained at identical concentration (= 5 mM) for all binary mixtures with unsaturated phospholipid. A minimum size at 5 mM is also observed for drug surfactant-DMPC mixtures but with significantly larger vesicle radii (14–16 nm). In drug surfactant-DPPC mixtures, the vesicles were always too large for their size to be determined from our SANS data (*i.e.* vesicle radius larger than about 50 nm). The overall drug-phospholipid concentration of 5 mM, where the vesicles appear to reach a minimum size, corresponds to rather high mole fractions of phospholipid in the vesicles ($x_{PL} \approx 0.8$).

The spontaneous formation of vesicles have been rationalized with bending elasticity theory combined with solution thermodynamics. The difference in aggregate phospholipid mole fraction at the point of micelle-to-bilayer transition indicates lower spontaneous curvature of the two unsaturated phospholipids DOPC and DEPC as compared with the saturated lipids DMPC and DPPC. Considering both AMT and DXP series with four different phospholipids, we may conclude that spontaneous curvature increases according to the following sequence DEPC < DOPC < [DPPC and DMPC]. On the other hand, the conspicuous difference in vesicle size between the different phospholipids appears to be a consequence of lower bending rigidity k_c for unsaturated phospholipids, despite having a larger hydrophobic moiety. A possible explanation for this is a reduced flexibility of the aliphatic hydrocarbon tails due to the presence of double bonds [31]. Likewise, a minimum size at some optimal drug/phospholipid composition in unilamellar vesicles may be rationalized as a result of the reduction of k_c upon mixing two amphiphilic components with different spontaneous curvatures. However, more experimental studies are needed to fully grasp this seemingly peculiar behavior. By comparing the minimum vesicle size for each phospholipid, we can arrange the phospholipids in ascending order of bending rigidity as follows: DOPC $\leq$ DEPC $<$ DMPC $<$ DPPC. The method of comparing bending rigidity for a set of phospholipids presented here can guide a unique approach for comparing bending rigidities of a group of amphiphiles with different molecular structures. Our present results may pave the way for more efficient utilization of phospholipids in tailor-made lipid formulations and lipid nano-carriers.

The spontaneously formed small and ultrasmall liposomal vesicles are stable as long we have observed them and much resembles unilamellar vesicles formed in mixtures of oppositely charged surfactants. Similar to the latter case, mixed drug surfactant-phospholipid vesicle mixtures appears to be thermodynamically stable. Hence, our mixtures of spontaneously formed vesicles behave as thermodynamically stable (1-phase) colloidal solutions such as micellar and microemulsion solutions, but are fundamentally different from metastable nonequilibrium (2-phase) colloidal dispersions of emulsions and nonequilibrium liposomes.

CRediT authorship contribution statement

Vahid Forooqi Motlaq: Writing – original draft, Visualization, Methodology, Investigation, Formal analysis, Conceptualization. **Lars Gedda:** Writing – review & editing, Visualization, Resources, Data curation. **Katarina Edwards:** Writing – review & editing, Resources. **James Doutch:** Data curation. **L.M. Bergström:** Writing – review & editing, Writing – original draft, Validation, Supervision, Resources, Project administration, Methodology, Investigation, Formal analysis, Data curation, Conceptualization.

Declaration of competing interest

The authors declare the following financial interests/personal relationships which may be considered as potential competing interests: Magnus Bergstrom reports financial support was provided by Uppsala University. Vahid Forooqi Motlaq reports was provided by Uppsala University. James Doutch reports financial support was provided by ISIS Pulsed Neutron and Muon Source. Lars Gedda reports financial support was provided by Uppsala University. Katarina Edwards reports financial support was provided by Uppsala University. If there are other authors, they declare that they have no known competing financial interests or personal relationships that could have appeared to influence the work reported in this paper.

Acknowledgments

This study is part of the science programs of the Swedish Drug Delivery Center (SweDeliver) with financial support from Vinnova (Dnr 2017-02690 and Dnr 2019-00048). The authors are also grateful the Faculty of Pharmacy at Uppsala University for financial support. We are also thankful to Sana Tirgani for the help with CMC measurements. Vahid Forooqi Motlaq is thankful to Erik Agner (Polypure AS) for his support during the writing process. The authors acknowledge the ISIS Neutron and Muon Source for provided beamtime with experiment number RB2210079 (DOI: 10.5286/ISIS.E.RB2210079-1).

Appendix A. Supplementary material

Supplementary data to this article can be found online at https://doi.org/10.1016/j.jcis.2024.12.098.

Data availability

Raw data is available online.

References

[1] M. Rostoff (Ed.), Vesicles, Surfactant Science Series, CRC Press, 1996.
[2] E.W. Kaler, et al., Spontaneous vesicle formation in aqueous mixtures of single-tailed surfactants, Science 245 (1989) 1371–1374.
[3] J.S. Pedersen, S.U. Egelhaaf, P. Schurtenberger, Formation of polymerlike mixed micelles and vesicles in lecithin-bile salt solutions: a small-angle neutron scattering study, J. Phys. Chem. 99 (1995) 1299–1305.
[4] D. Lichtenberg, E. Opatowski, M.M. Kozlov, Phase boundaries in mixtures of membrane-forming amphiphiles and micelle-forming amphiphiles, BBA 1508 (2000) 1–19.
[5] V. Forooqi Motlaq, et al., Investigation of the enhanced ability of bile salt surfactants to solubilize phospholipid bilayers and form mixed micelles, Soft Matter 17 (2021) 7769–7780.
[6] M. Almgren, Mixed micelles and other structures in the solubilization of bilayer lipid membranes by surfactants, BBA 1508 (2000) 146–163.
[7] M. Bergström, J.S. Pedersen, A small-angle neutron scattering study of surfactant aggregates formed in aqueous mixtures of sodium dodecyl sulfate and didodecyldimethylammonium bromide, J. Phys. Chem. B 104 (2000) 4155–4163.
[8] V. Forooqi Motlaq, et al., Spontaneous formation of ultrasmall unilamellar vesicles in mixtures of an amphiphilic drug and a phospholipid, Langmuir 39 (32) (2023) 11337–11344.
[9] L.M. Bergström, Thermodynamics of self-assembly, in: M. Tadashi (Ed.), Application of Thermodynamics to Biological and Material Science, InTech, Rijeka, 2011, pp. 289–314.
[10] W. Helfrich, Elastic properties of lipid bilayers: theory and possible experiments, Zeitschrift Für Naturforschung C 28 (1973) 693–703.
[11] S.A. Safran, P. Pincus, D. Andelman, Theory of spontaneous vesicle formation in surfactant mixtures, Science 248 (1990) 354.
[12] M.M. Kozlov, W. Helfrich, Effects of a cosurfactant on the stretching and bending elasticities of a surfactant monolayer, Langmuir 8 (1992) 2792–2797.
[13] G. Porte, C. Ligoure, Mixed amphiphilic bilayers: bending elasticity and formation of vesicles, J. Chem. Phys. 102 (1995) 4290–4298.
[14] L.M. Bergström, Bending elasticity of charged surfactant layers: the effect of mixing, Langmuir 22 (2006) 6796–6813.
[15] D. Lichtenberg, Characterization of the solubilization of lipid bilayers by surfactants, Biochimica et Biophysica Acta (BBA)-Biomembranes 821 (3) (1985) 470–478.
[16] L.M. Bergström, M. Aratono, Synergistic effects in mixtures of two identically charged ionic surfactants with different critical micelle concentrations, Soft Matter 7 (19) (2011) 8870–8879.
[17] V. Forooqi Motlaq, et al., Investigation of the enhanced ability of bile salt surfactants to solubilize phospholipid bilayers and form mixed micelles, Soft Matter 17 (33) (2021) 7769–7780.
[18] D. Attwood, S.P. Agarwal, Investigation of the self-association of an amphiphilic drug in aqueous solution, J. Chem. Soc., Faraday Trans. 1 76 (1980) 570–577.
[19] ZOOM diffractometer at the ISSI neutron source, https://www.isis.stfc.ac.uk/Pages/Zoom.aspx.
[20] P. Lindner, T. Zemb, Neutron, X-ray and Light Scattering: Introduction to an Investigative Tool for Colloidal and Polymeric Systems, North-Holland, Netherlands, 1991.
[21] http://www.mantidproject.org/Main_Page.
[22] J.S. Pedersen, Analysis of small-angle scattering data from colloids and polymer solutions: modeling and least-squares fitting, Adv. Colloid Interface Sci. 70 (1997) 171–210.
[23] L.M. Bergström, Bending energetics of tablet-shaped micelles: a novel approach to rationalize micellar systems, ChemPhysChem 8 (3) (2007) 462–472.
[24] L.M. Bergström, Explaining the growth behavior of surfactant micelles, J. Colloid Interface Sci. 440 (2015) 109–118.
[25] L. Magnus Bergström, Second CMC in surfactant micellar systems, Curr. Opin. Colloid Interface Sci. 22 (2016) 46–50.
[26] L. Arleth, M. Bergström, J.S. Pedersen, Small-angle neutron scattering study of the growth behavior, flexibility, and intermicellar interactions of wormlike SDS micelles in NaBr aqueous solutions, Langmuir 18 (14) (2002) 5343–5353.
[27] N. Kučerka, S. Tristram-Nagle, J.F. Nagle, Structure of fully hydrated fluid phase lipid bilayers with monounsaturated chains, J. Membr. Biol. 208 (2006) 193–202.
[28] J.F. Nagle, S. Tristram-Nagle, Structure of lipid bilayers, Biochim. Biophys. Acta (BBA)-Rev. Biomembr. 1469 (3) (2000) 159–195.
[29] L.M. Bergström, Model calculations of the spontaneous curvature, mean and Gaussian bending constants for a thermodynamically open surfactant film, J. Colloid Interface Sci. 293 (2006) 181–193.
[30] M.K. Dymond, Lipid monolayer spontaneous curvatures: a collection of published values, Chem. Phys. Lipids 239 (2021) 105117.
[31] L.M. Bergström, Bending elasticity of charged surfactant layers: the effect of layer thickness, Langmuir 22 (2006) 3678–3691.
[32] B. Kollmitzer, et al., Monolayer spontaneous curvature of raft-forming membrane lipids, Soft Matter 9 (45) (2013) 10877–10884.
[33] M. Kaltenegger, et al., Intrinsic lipid curvatures of mammalian plasma membrane outer leaflet lipids and ceramides, Biochim. Biophys. Acta (BBA) - B Biomembr. 1863 (11) (2021) 183709.
[34] J. Pan, et al., Temperature dependence of structure, bending rigidity, and bilayer interactions of dioleoylphosphatidylcholine bilayers, Biophys. J. 94 (1) (2008) 117–124.